VERSITA

INTERNATIONAL
Agrophysics
www.international-agrophysics.org

Int. Agrophys., 2013, 27, 211-218
doi: 10.2478/v10247-012-0087-6

Electrical resistivity tomography to delineate greenhouse soil variability**

R. Rossi[1], *M. Amato*[2]*, *G. Bitella*[2], *and R. Bochicchio*[3]

[1]CRA-SCA, Via Celso Ulpiani, 5, 70125 Bari, Italy
[2]School of Agriculture, Forest, Food and Environmental Sciences, University of Basilicata Viale dell'Ateneo Lucano, 85100 Potenza, Italy
[3]International Doctoral School: Crop Systems, Forest, Food and Environmental Sciences, University of Basilicata, Viale dell'Ateneo Lucano, 85100 Potenza, Italy

Received March 2, 2012; accepted February 18, 2013

A b s t r a c t. Appropriate management of soil spatial variability is an important tool for optimizing farming inputs, with the result of yield increase and reduction of the environmental impact in field crops. Under greenhouses, several factors such as non-uniform irrigation and localized soil compaction can severely affect yield and quality. Additionally, if soil spatial variability is not taken into account, yield deficiencies are often compensated by extra-volumes of crop inputs; as a result, over-irrigation and over-fertilization in some parts of the field may occur. Technology for spatially sound management of greenhouse crops is therefore needed to increase yield and quality and to address sustainability. In this experiment, 2D-electrical resistivity tomography was used as an exploratory tool to characterize greenhouse soil variability and its relations to wild rocket yield. Soil resistivity well matched biomass variation (R^2=0.70), and was linked to differences in soil bulk density (R^2=0.90), and clay content (R^2=0.77). Electrical resistivity tomography shows a great potential in horticulture where there is a growing demand of sustainability coupled with the necessity of stabilizing yield and product quality.

K e y w o r d s: electrical resistivity tomography, yield variability, greenhouse, soil spatial variability

INTRODUCTION

Wild rocket (*Diplotaxis tenuifolia* L.) is a multifunctional species of the Brassicaceae family, used in traditional pharmacopoeia for its several therapeutic properties: depurative, tonic, and anti-inflammatory. It is also used as an ingredient in salads and cooked dishes, and it is appreciated for its pungent flavour and nutraceutical properties linked to health-promoting agents such as flavonoids and glucosinolates, associated with a reduced risk of several types of cancer and cardiovascular diseases (Jin *et al.*, 2009). The economic potential of wild rocket has been greatly enhanced by the introduction in the market of the so-called 4th Generation vegetables. The quality of this type of fresh vegetables, marketed after leaf cutting and cleaning, is an essential component of their price. Leaf size, colour and other quality traits can be greatly affected by the spatial variability of growing conditions, such as non-uniform irrigation and localized soil compaction. The resulting variability in crop yield and other characteristics is usually managed by increasing crop inputs, and therefore over-irrigation and over-fertilization in some parts of the field may occur (de Tourdonnet *et al.*, 2001). The consequences are threefold:

- the efficiency of inputs is reduced, and water, money and energy are wasted;
- product safety is at risk because of accumulation of potentially harmful compounds;
- the environmental impact increases due to soil pollution and leaching of nutrients.

Overuse or misuse of nitrogen (N) fertilizers and pesticide leaching have long been recognized as a serious environmental concern in intensive greenhouse systems; therefore, strategies for decreasing the rate of traditional N fertilizers without yield losses are actively pursued. A life-cycle assessment by Munoz *et al.* (2008) shows that a reduction of 36% in N fertilizers can reduce the potential impact of eutrophication by 60%, and can decrease the potential impact of climate change by 50% and the potential impact of photochemical oxidants by 45%.

*Corresponding author e-mail: marinria@gmail.com
**This work was partly funded by the EC-InterregIIIBWETMUST project, 2010-2013.

A sound alternative to overuse of inputs to compensate for the spatial variability of the growing medium, or to a uniform reduction of inputs to minimize environmental impact would be site-specific management of greenhouse crops.

Tools for fast and effective acquisition of information for the spatially sound management of crops have been developed and tested in field settings (Rossi *et al.*, 2011), but information on the performance of techniques for assessing the spatial variability of the growth media in greenhouses is lacking.

The measurement of apparent soil electrical resistivity (ER) or its inverse (apparent electrical conductivity) has proved to be a promising non-destructive tool to delineate soil spatial variation at different scales (Samouelian *et al.*, 2005). ER is measured by injecting a direct current (DC) electric current through the ground *via* a pair of electrodes; the resulting potential difference is measured between the second pair of electrodes. When current is injected in a homogeneous isotropic medium, it flows radially and symmetrically in the half space below the electrodes. Resistivity (ρ = Ohm m) is defined by the following expression:

$$\rho = 2\pi \frac{\Delta V}{I} K ,$$

where: ΔV is the potential difference (V), I is the current intensity (A) and K is the so-called geometrical factor that depends on electrode arrangement. Each set of four electrodes (quadrupole) yields a single value of resistivity attributed to a volume of soil with dimension and depth depending on the inter-electrode spacing. The electrodes can be positioned in several configurations characterized by a different imaging ability (Dahlin and Zhou, 2004). Two-dimensional electrical resistivity tomography (ERT) surveys are conducted using a large number of electrodes connected to a multicore cable. An electronic switching unit automatically selects a single quadrupole at a time along the line, progressively increasing the distance between electrodes, to explore different soil volumes and layers (Fig. 1). Soil resistivity obtained from the surveys is calculated assuming soil homogeneity; it is known as 'apparent' resistivity and is usually displayed in a vertical section called pseudo-section (Fig. 1b). Soil heterogeneity, causes a deformation of the current flow lines, and therefore apparent resistivity values are not correctly located in space. Numerical treatment (inversion) of data is then required to yield 'true' resistivity with correct spatial distribution represented in a section called tomogram (Fig. 1d). Resistivity measurements were initially introduced in agriculture for measuring soil salinity. Over the last decade resistivity has been extensively used to characterize soil variability and system dynamics at several scales from centimetres to landscapes (Basso *et al.*, 2010; Besson *et al.*, 2010; Samouelian *et al.*, 2003), thanks to its reliability, ease of measurement, and the correlation with several soil properties such as texture, bulk density and water content. The potential of ERT in horticulture has not been exploited yet.

The objective of this study is to use 2-D electrical resistivity tomography to reveal the sources of variability in a greenhouse-grown rocket crop, where spatial variation of biomass

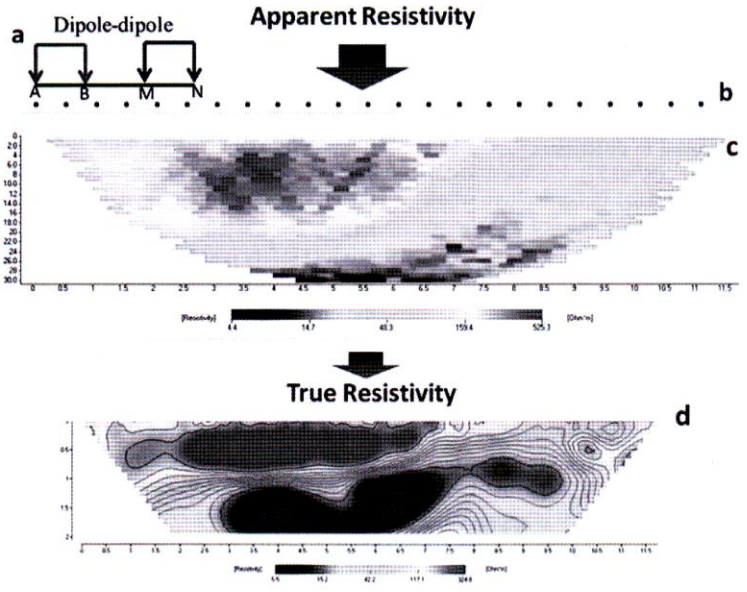

Fig. 1. 2D – electrical resistivity tomography; a – arrangement of current (A, B) and potential (M, N) electrodes in the dipole-dipole array; b – position of multi electrode arrays on soil surface; c – 2D pseudo section (apparent resistivity data) obtained after data acquisition; d – 2D tomogram (true resistivity data) obtained after data inversion with numerical modelling.

was found. More specifically, we tested two hypotheses: that the variation in crop performance corresponded to the variation in electrical resistivity of the growth medium, and that the resistivity was related with soil properties linked to management.

MATERIALS AND METHODS

The study was conducted in a standard plastic module greenhouse located in Pontecagnano Faiano (Salerno, Italy).

The tunnel dimensions were 7.20 x 33.68 m. The tunnel cover was a stabilized opalescent thermal Polyethylene sheet of 2 mm. The sprinkler irrigation system consisted of 2 parallel lines 2 m height per tunnel set at a distance of 3.60 m and spaced at 2.5 m along the row, with an outflow rate of 132 l h^{-1}.

Wild rocket (*Diplotaxis tenuifolia* L.) was planted at a density of 1174 m^{-2} in beds of 1.3 m with inter-bed spaces of 0.3 m, and harvested by repeated cutting during the growing season (4 cuts per year). Conventional mineral fert-irrigation was supplied during each cut growing cycle at the following doses: N – 22.6, K_2O – 47.1, and P_2O_5 – 9.8 kg ha^{-1}, respectively. The experiment was performed at the time of the fourth harvest.

Two-dimension ERT was performed with an Iris Syscal Pro ten-channel resistivity meter (Iris Instruments, Orléans-France), on two soil transects:one parallel and the other perpendicular to the main tunnel axis (respectively, Transect A and B). All apparent-resistivity data were collected using a line of 48 steel electrodes spaced at 10 cm distance to give a total length of the line of 4.70 m and an exploration depth of 98 cm. The electrode configuration was dipole-dipole, where the distance d between electrodes used for current injection was the same as that between electrodes used for measuring voltage. The distance (d) between the current electrode pair and the potential electrode pair was progressively increased to explore subsequent soil layers at a depth multiple of d. Measurements were made using the minimum distance of $d = 10$ cm. A total of 1880 resistivity values were obtained from each transect. The dipole-dipole array was chosen because of its great sensitivity to horizontal variations in resistivity as reviewed by Dhalin and Zhou (2004). After acquisition, the data were inverted through a two-dimensional finite-element inversion algorithm implemented with the Tomolab inversion software (GeostudiAstier, Livorno Italy), and true resistivity values were obtained and displayed in tomograms (Figs 2 and 3). Tomograms were

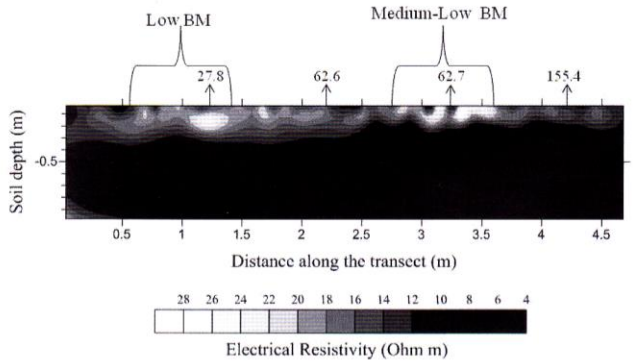

Fig. 2. 2D-electrical resistivity tomogram generated in Transect A; areas comprised within the braces show areas of low and medium-low rocket biomass (BM) values at visual assessment. Black arrows indicate sampling locations and corresponding fresh biomass values.

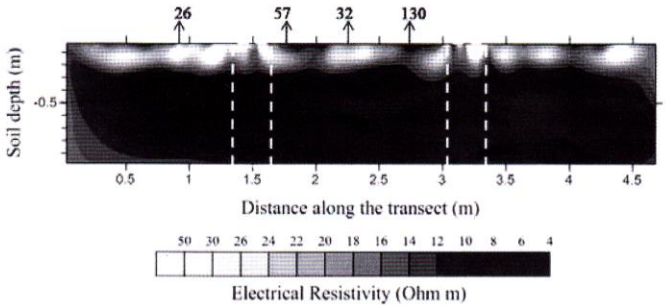

Fig. 3. 2D-electrical resistivity tomogram generated in Transect B; dotted lines indicate the inter-rows. Black arrows indicate sampling locations and corresponding fresh biomass values.

available in the field within 30 min from data acquisition and were used to identify eight locations of contrasting resistivity, which were selected for destructive sampling. In each location, soil samples were collected at 0.10 and 0.20 m depth in two locations. A total of 10 samples were available for laboratory determinations. Summary statistics of soil biophysical and chemical analysis are presented in Table 1. Soil dry bulk density (Bd) was determined at all sampling locations by the 'cylinder method' with cylinders of 0.10 m diameter and 0.12 m length. At each sampling location, vegetation was clipped to the soil surface within an area of 18x18 cm and weighted. Each sample was then oven dried at 70°C until constant weight and reweighed for gravimetric determination. Soil cores were used for root determinations after washing over a 0.2 mm square meshed sieve and after clay dispersion with a solution of hexametaphosphate (85%) and sodium bicarbonate (15%) at 10% (w/w) dilution (Amato *et al.*, 2008). Non-root materials were separated manually from washed samples, and root materials were weighed after drying at 70°C until constant weight. Root length was measured by scanning followed by image analysis with the WinRhizo software (Regent Instruments Inc., 1996). Root dry mass density was divided by above ground biomass dry weight to yield the root/shoot – ratio.

Univariate regression analysis was performed on resistivity data and variables from the destructive measurements. Analysis of variance (ANOVA) was performed on observations divided into two groups corresponding to resistivity lower and higher than 15 Ohm m (low resistive area, LR, and high resistive area, HR), respectively.

RESULTS AND DISCUSSION

Summary statistics for resistivity, soil variables and above- and below-ground biomass are presented in Table 1, and the spatial distribution of ER is shown in Figs 2, 3. Soil electrical resistivity measured in the two transects exhibits a large spatial variability.The tomogram for transect A reveals localized areas of highest resistivity (= resistive anomalies) a few decimetres long (light-grey to white shades in

Table 1. Descriptive statistics of ER and soil biophysical variables in destructive samples. ER – in-situ soil electrical resistivity; Θg – soil gravimetric water content, Bd – bulk density, BM – rocket biomass, RMD – root mass density, RLD – root length density

Parameters	Mean	Median	Standard deviation	Kurtosis	Skeweness	Range	Min	Max	$N_{samples}$
ER (Ohm m)	17.37	14.54	6.88	2.23	1.51	23.07	10.00	33.07	10
Bd (g cm^{-3})	1.22	1.22	0.05	0.96	-0.04	0.20	1.12	1.32	10
Θg (%, g g^{-1})	14.33	14.72	1.43	-1.59	-0.15	4.00	12.40	16.39	10
Fresh BM (g)	69.31	59.80	48.41	-0.06	1.12	129.20	26.20	155.40	8
Dry BM (g)	8.00	7.05	3.54	-0.26	0.94	9.70	4.60	14.30	8
RMD (g cm^{-3})	0.000066	0.000057	0.000046	-0.69	0.63	0.000138	0.000011	0.000149	10
RLD (cm cm^{-3})	0.89	0.98	0.26	1.28	-1.21	0.84	0.35	1.19	9
Sand (%, g g^{-1})	29.67	29.83	0.78	0.91	0.00	2.85	28.28	31.14	10
Silt (%, g g^{-1})	30.61	30.59	2.48	-0.85	-0.23	7.71	26.30	34.01	10
Clay (%, g g^{-1})	39.73	39.63	1.81	-0.86	0.01	5.84	36.79	42.63	10
pH	8.2	8.2	0.1	-0.3	-0.6	0.3	8.0	8.3	10
Carbonate (%, g g^{-1})	1.28	1.20	0.38	1.11	0.92	1.32	0.75	2.08	10
SO (‰, g g^{-3})	10.03	9.58	2.75	-0.61	0.55	8.49	6.52	15.01	10
N (‰, g g^{-3})	1.07	1.06	0.06	-1.49	-0.14	0.17	0.98	1.15	10
P_2O_5 (mg kg^{-1})	39.25	39.05	11.13	0.02	-0.01	37.80	20.60	58.40	10
K_2O (mg kg^{-1})	665.78	682.93	92.65	-1.18	-0.22	269.23	533.10	802.33	10
CSC (mol Kg^{-1})	0.263	0.263	0.008	1.562	0.902	0.030	0.251	0.281	10
Ca (mol Kg^{-1})	0.093	0.092	0.002	0.669	0.985	0.007	0.090	0.098	10
Mg (mol Kg^{-1})	0.013	0.013	0.000	1.357	0.982	0.001	0.013	0.014	10
K (mol Kg^{-1})	0.014	0.014	0.002	-1.182	-0.223	0.006	0.011	0.017	10
Na (mol Kg^{-1})	0.038	0.037	0.002	1.013	0.786	0.007	0.035	0.042	10

Fig. 2). Soil resistivity decreases with increasing depth, and a low-resistivity area (medium-grey to black shades) is found between 0.75 and 3.75 m from the starting point of the transect. The depth of this area ranges from 0.6 m from the soil surface (left side of tomogram) to 0.2 m (right side of the tomogram).

The resistivity pattern displayed in Fig. 3 for transect B consists in the presence of narrow bands of low resistivity at the edges of beds, whereas higher resistivity was found in the bed centre. The highest values of resistivity (60 Ohm m) are found in the inter-bed where the soil was dry and fissured by large cracks.

In both transects, the resistivity patterns match biomass variations, and areas of higher resistivity are located corresponding to areas of lower biomass.

When true resistivity values were compared quantitatively with rocket biomass at the sampled locations with the analysis of variance, biomass was significantly lower ($p<0.05$) in the HR areas (Fig. 4).

A significant power relationship ($y= 340.7\ x^{-1.39}$, $p<0.009$) was found between average resistivity in the first 30 cm and above-ground biomass, with the coefficient of determination 0.70 (Fig. 5).

The ratio of root to shoot biomass matches resistivity distribution in both transects (Fig. 6), highest values were found in resistive areas. The proportion of crop assimilate partitioned to roots, expressed by the ratio of root to shoots biomass, is part of the adapting strategies of plants. An increase in the root/shoot ratio is often a response to unfavourable growing conditions; therefore, we may interpret the direct relationship between this index and ER in our transects as a further indication that high resistivity identifies areas of poor quality in the growth medium.

The relationships between resistivity and soil variables are different between the two transects. In transect A resistivity is significantly correlated to clay variation (Fig. 7 b, $R^2 = 0.77$) and this is consistent with the literature (Samouelian *et al.*, 2005). Electrical resistivity is very sensitive to the presence of clay particles, since the diffuse double layer at the clay surface has remarkable conducting properties. In the literature, clay minerals are generally put in a single group within a resistivity range from 1 to 100 Ohm m (Samouelian *et al.*, 2005). However, experimental results on saturated clays have shown that resistivity is extremely high (in the order of hundreds Ohm m) only for a very low water content (<10%). ER values abruptly drop to values of around 10 Ohm m atthewater content higher than around 20%, because of continuity of pore water (Fukue *et al.*, 1999). Resistivity measured on clay samples collected worldwide varies in a very narrow range (from 1 to 12 Ohm m), and this conductive behaviour makes clayey horizons clearly discernible from overlaying silty and sandy soil layers (Giao *et al.*, 2003). In our case, values of 12 Ohm m and lower were found below 30 cm, with some horizontal variation, and can be attributed to the presence of clay. Slight differences in the clay content were also measured between areas of contrasting resistivity within the surface layer in transect A. This surface variation might be linked to localized detachment and sorting of fine particles that occurs during irrigation.

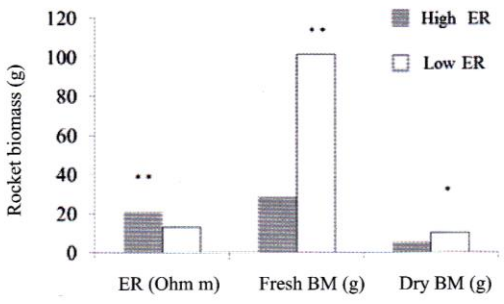

Fig. 4. Soil electrical resistivity (ER), fresh and dry rocket biomass (BM) averaged in areas of high and low resistivity, *p <0.06, **p <0.05.

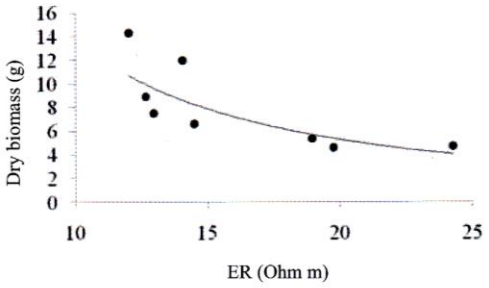

Fig. 5. Plot of soil electrical resistivity (ER) averaged in the 0-30 cm soil layer and dry rocket biomass measured in the two transects, $p<0.009$.

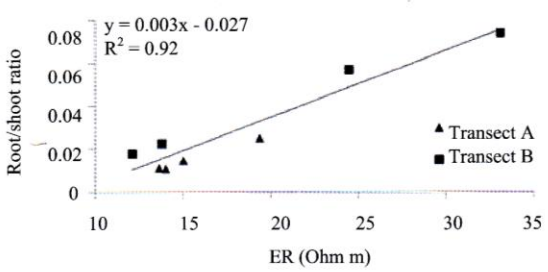

Fig. 6. Soil electrical resistivity (ER) and root/shoot ratio.

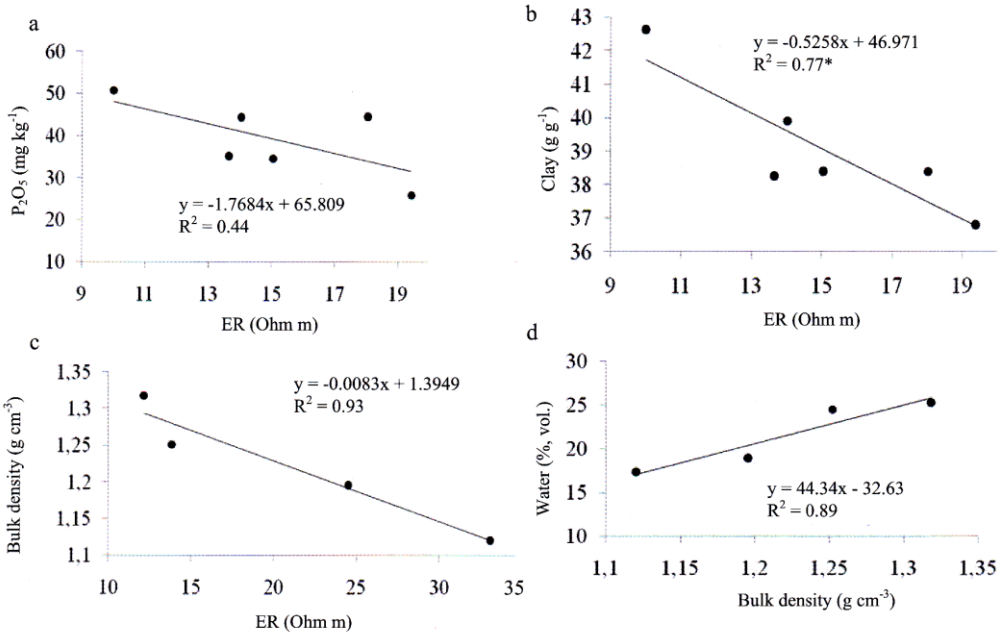

Fig. 7. Electrical resistivity (ER) and soil parameters in transect A (a, b) and in transect B (c, d): a – P_2O_5 versus ER; b – clay content versus ER; c – bulk density versus ER; d – volumetric water content versus bulk density, $p < 0.05$.

In our study, resistivity also shows a negative but non-significant correlation with available P and K (Fig. 7 a). Phosphate and potassium are more variable than texture or other variables (Table 1), and they are correlated with each other and positively correlated with the clay content ($r = 0.87$ and $r = 0.83$, respectively). Some studies demonstrate that field measurements of soil electrical conductivity (ECa) are well related to the content of ions, and therefore can be used to predict the availability of soil nutrients. Sudduth *et al.* (2005) conducted investigations of the relations between soil properties and ECa and showed that the correlation of ECa with the clay content and cation exchange capacity (CEC) tends to be high and consistent across soil types, and even at different times of the year, in soils with variable water content and subjected to different management. High correlations of ECa with the K^+ and Mg^{2+} concentration in the saturated extract have also been reported by Corwin and Lesch (2005). As reported above, in our study, the areas of low biomass correspond to limited P availability. It is well known that plants subjected to P deficiency undergo changes in energy metabolism *ie* they exhibit a decrease in the respiration rate and ATP synthesis. Phosphorus starvation limits biomass growth by interfering with nitrate uptake, and assimilate partitioning between shoots and roots (De Groot *et al.*, 2003). In our experimental setting, a variable distribution of P and other nutrients in the top-soil can be attributed to differences in plant water/ion uptake or to non-uniform irrigation. In transect A, the spatial pattern of ER in the surface layer revealed a systematic 'wavy' trend parallel to the irrigation pipes. This suggests malfunctioning in the sprinkle irrigation system.Uniformity in the distribution of water and nutrients through fertirrigation may be a problem in greenhouse settings; systems are often designed so that the area watered by each sprinkler largely overlaps the area watered by the adjacent sprinkler, but overlapping may be insufficient due to pressure deficits or partial to total clogging of sprinkler heads. Consequently, localized spots of soil with insufficient water and fertilizers supply are common. Plugging of emitters has been recognized as one of the most serious maintenance problems that frequently lower greenhouse product quality.

Clogging can be caused by several biological, physical, or chemical factors (Kreij *et al.*, 2003), but it is difficult to identify clogged emitters: measuring irrigation uniformity at the field scale is laborious and only gives information on global uniformity. Soil-water status sensors such as tensiometers, capacitive sensors, or neutron scattering may be used to monitor the performance and uniformity of irrigation systems. Such methods, though, are 1-dimensional and small-scale, since they provide information within a region of a few centimetres from the probe; therefore, they poorly cover the

spatial distribution of water (Schwartz *et al.*, 2008). Furthermore, soil sensors cannot discern whether water has been drained, up-taken by plants, or redistributed within the root zone and thus it is difficult to translate this kind of data into irrigation decisions. Stirzaker (2003) has demonstrated that wetting front monitoring is more useful for irrigation management and monitoring of leaching processes. Even in this case, however, point measuring devices are needed, and, in the absence of knowledge on the spatial structure of soil variation, it is difficult to judge how representative they are of the surrounding soil regions.

ER tomography can help address such issues in several ways: it can directly measure the spatial distribution of water and reveal hydrological dynamics if used for sequential measurements of the same profile. In addition, 2-D or 3-D coverage provides information on soil spatial variability to be used as a basis for the correct placement of traditional sensors (Amato *et al.*, 2008).

In transect B (Fig. 3), resistivity distribution matches the biomass content, as in transect A, but neither biomass nor ER are linked to texture or nutrient availability; rather, a strong positive correlation of ER with soil bulk density was found (Fig. 7c). Resistivity is sensitive to the bulk density of soils and to any other index related to soil structure, such as porosity, because the relative amount of voids and solids affects the ability of soil volumes to conduct electrical currents. The electrical resistivity of air is virtually infinite; therefore, a dry porous soil is in general more resistive than a compacted one. Besson *et al.* (2004) used surface two-dimensional ER tomography with the same settings as those adopted in our study to map soil structure in tilled layers. In their tomograms, soil compaction resulting from wheel traffic was clearly detected, and the plough pan was visible. They found that electrical resistivity decreases with increasing bulk density following a non-linear relationship. A difference of 11 Ohm m was found between compacted areas (average bulk density of 1.59 Mg m^{-3}) and porous soil blocks (bulk density of 1.39 Mg m^{-3}), and the bulk density was also positively correlated with the volumetric water content. In other studies, loose soil was associated with values around 50 Ohm m, whereas soil cracks produced large peaks in resistivity (Seger *et al.*, 2009). The high sensitivity of resistivity to even small voids has also been documented by Samouelian *et al.* (2003), who detected soil cracks at the centimetre scale with a miniaturized resistivity tomography setting. ERT is also sensitive enough to soil structure to detect the effect of different tillage systems on soils, possibly due to different aggregate dimensions (Basso *et al.*, 2010). In our study, when overall bulk density values were regressed against resistivity, all the observations collected in transect A were tightly clustered around the regression line calculated for transect B. Only one observation fell far from the trend line and corresponded to a sample where the high clay content reduced resistivity. In transect B, bulk density is also positively correlated with rocket biomass. Bulk density is positively correlated with the gravimetric water content and more strongly with the volumetric water content (Fig. 7d).

Areas of high resistivity in transect B, corresponding to unfavourable conditions for rocket growth, may therefore be ascribed to low bulk density, with the lowest values (Bd< 1.20 g cm^{-3}) in the middle of the bed.

In our experiment, the beds were prepared for planting with a traditional convex shaping of the soil surface called 'baulatura'. This creates a slight slope between the centre and the edges of each bed to avoid water logging, but may also cause differential compaction of the bed edges compared to the centre.

In a review of the effects of soil condition on plant growth, Passioura (2002) has shown that plant performance is impaired by excessive compaction, but plants can grow poorly in loose soil as well: at a bulk density below 1.20 g cm^{-3} barley shoot weight was about 15% less than at optimal bulk density. The author reports that growth reduction was associated with the presence of large soil pores and argues that this response might be explained by poor root-soil contact, with negative consequences on seedling establishment and plant water uptake. In addition to water and nutrient shortage, roots growing in physically inhospitable media send inhibitory signals to the shoots with long-term effects on growth.

In our exploratory study, ER tomography allowed detection of soil patterns related to the above- and below-ground biomass in the wild rocket, possibly linked to inadequate management of soil structure and irrigation, but the potential of resistivity tomography goes far beyond. Our results demonstrate that heterogeneity in the soil status large enough to affect yield can be generated in greenhouse management, and therefore, attention must be paid to seedbed preparation, soil structural status, and irrigation systems operation.

The scale of measurements we used lends itself to a rather immediate extension to fast plot-scale and greenhouse-scale applications with the use of systems for continuous measurement of ER or ECa (Basso *et al.*, 2010; Corwin and Lesch, 2005). Such on-the-go systems cover hectares in a day of work andexplore soil volumes from the top few decimetres down to approximately two-meter depth, therefore from the root zone to shallow water tables. High resolution data relevant to root zone dynamics can be collected this way and can be used to calibrate crop simulation models and extend 1-dimensional predictions to the entire greenhouse in a spatially sound way.

CONCLUSIONS

1. Exploratory analysis demonstrated that small spatial scale soil variability could be clearly delineated by electrical resistivity tomography and that this variability well matched the patterns of above- and below-ground biomass of a horticultural crop.

2. Electrical resistivity tomography allowed detecting soil patterns possibly linked to inadequate management of soil structure and irrigation. Significant correlations were found with bulk density and clay content.

3. Electrical resistivity tomography can help overcome limits associated to 1-Dimensional management technologies by providing a 2D or 3D data coverage that can be used to infer hydrological dynamics as a feedback for tillage operations and seedbed preparation and as a basis for correct placement of traditional sensors.

REFERENCES

Amato M., Basso B., Celano G., Bitella G., Morelli G., and Rossi R., 2008. In situ detection of tree root distribution and biomass by multielectrode resistivity imaging. Tree Physiol., 28, 1441-1448.

Basso B., Amato M., Bitella G., Rossi R., Kravchenko A., Sartori L., Carvalho M.L., and Gomes J., 2010. Two dimensional spatial and temporal variation of soil physical properties in tillage systems using electrical resistivity tomography. Agronomy J., 102(2), 440-449.

Besson A., Cousin I., Bourennane H., Nicoullaud B., Pasquier C., Richard G., Dorigny A., and King D., 2010. The spatial and temporal organization of soil water at the field scale as described by electrical resistivity measurements. Eur. J. Soil Sci., 61, 120-132.

Besson A., Cousin I., Samouelian A., Boizard H., and Richard G., 2004. Structural heterogeneity of the soil tilled layer as characterized by 2D electrical resistivity surveying. Soil Till. Res., 79, 239-249.

Corwin D.L. and Lesch S.M., 2005. Characterizing soil spatial variability with apparent soil electrical conductivity Part II. Case study. Computers Electronics Agric., 46, 135-152.

Dahlin T. and Zhou B., 2004. A numerical comparison of 2D resistivity imaging with 10 electrode arrays. Geophys. Prospecting, 52, 379-398.

De Groot C.C., Marcelis L.F.M., van den Boogaard R., Kaiser W.M., and Lambers H., 2003. Interaction of nitrogen and phosphorus nutrition in determining growth. Plant Soil, 248, 257-268.

De Tourdonnet S., Meynard J.M., Lafolie F., Roger-Estrade J., Lagier J., and Sebillotte M., 2001. Non-uniformity of environmental conditions in greenhouse lettuce production increases the risk of N pollution and lower product quality. Agronomie, 21(4), 297-310.

Fukue M., Minatoa T., Horibe H., and Taya N., 1999. The micro-structure of clay given by resistivity measurements. Eng. Geol., 54, 43-53.

Giao P.H., Chung S.G., Kim D.Y., and Tanaka H., 2003. Electric imaging and laboratory resistivity testing for geotechnical investigation of Pusan clay deposits. J. Appl. Geophy., 52, 157-175.

Jin J., Koroleva O.A., Gibson T., Swanston J., Magan J., Zhang Y., Rowland I.R., and Wagstaff C., 2009. Analysis of phytochemical composition and chemoprotective capacity of rocket (*Erucasativa* and *Diplotaxistenuifolia*) leafy salad following cultivation in different environments. J. Agric. Food Chem., 57, 5227-5234.

Kreij C., van der Burg A.M.M., and RuniaW.T., 2003. Drip irrigation emitter clogging in Dutch greenhouses as affected by methane and organic acids. Agric. Water Manag., 60(2), 73-85.

Munoz P., Antón A., Paranjpe A., Arino J., and Montero J.I., 2008. High decrease in nitrate leaching by lower N input without reducing greenhouse tomato yield. Agron. Sust. Develop., 28, 489-495.

Passioura J.B., 2002. Soil conditions and plant growth. Plant, Cell Environ., 25, 311-318.

Rossi R., Amato M., Bitella G., Bochicchio R., Ferreira Gomes J.J., Lovelli S., Martorella E., and Favale P., 2011. Electrical resistivity tomography as a non-destructive method for mapping root biomass in an orchard. Eur. J. Soil Sci., 62, 206-215.

Samouelian A., Cousin I., Richard G., Tabbagh A., and Bruand A., 2003. Electrical resistivity imaging for detecting soil cracking at the centimetric scale. Soil Sci. Soci. J. Am., 67, 1319-1326.

Samouelian A., Cousin I., Tabbagh A., Bruand A., and Richard G., 2005. Electrical resistivity survey in soil science: A review. Soil Till. Res., 83, 173-193.

Schwartz B., Schreiber M., and Yan T., 2008. Quantifying field-scale soil moisture using electrical resistivity imaging. J. Hydrol., 362(3-4), 234-246.

Séger M., Cousin I., Frison A., Boizard H., and Richard G., 2009. Characterisation of the structural heterogeneity of the soil tilled layer by using in situ 2D and 3D electrical resistivity measurements. Soil Till. Res., 103(2), 387-398.

Stirzaker R.J., 2003. When to turn the water off: scheduling microirrigation with a wetting front detector. Irrig. Sci., 22, 177-185.

Sudduth K.A., Kitchen N.R., Wiebold W.J., Batchelor W.D., Bollero G.A., Bullock D.G., Clay D.E., Palm H.L., Pierce F.J., Schuler R.T., and Thelen K.D., 2005. Relating apparent electrical conductivity to soil properties across the North-Central USA. Comp. Electron. Agric., 46, 263-283.